# ENCAPSULATED BREAKER RELEASE RATE AT HYDROSTATIC PRESSURE AND ELEVATED TEMPERATURES

Sho-Wei Lo, Matthew J. Miller, and Jack Li
Schlumberger

## ABSTRACT

Encapsulated breakers for water-based fracturing fluids have been widely used for the past decade. These breakers provide a delayed break because the reactive chemical is separated from the fracturing fluid by a water-resistant coating. Higher breaker concentrations can be used, resulting in improved proppant pack conductivity. However, the coating is not completely impermeable. The breaker material can release through the coating under certain conditions when placed in an aqueous environment.

This paper shows the breaker release rate as a function of temperature, hydrostatic pressure and aqueous fluid pH. A breaker release apparatus was developed, and tests were performed from 150°F to 225°F, 0 to 8000 psig, and fluid pH of 4, 7, and 9.5. The major findings were that the breaker release rate is a very strong function of pressure and temperature, but is independent of aqueous fluid pH. Fifteen percent of the encapsulated breaker is released after 6 hours at 150°F and 0 psig, whereas only 8% and 7% of the breaker is released at 2000 psig and 8000 psig, respectively. Sixty percent of the breaker is released after 1 hour at 225°F and 500 psig, while the 8000 psig breaker release is 12% after 1 hr. These findings suggest that tests evaluating the stability of fracturing fluids at low hydrostatic pressure conditions (such as using Model 35 or Model 50 rheometers) do not represent the actual breaker performance under fracturing conditions. Breaker schedules based on these low-pressure tests underuse encapsulated breakers and jeopardize the proppant pack cleanup process. Using the correlations developed in this study, it is possible to calculate the wellsite breaker schedule from low-pressure rheology tests using encapsulated breakers. Polymer-induced fracture damage will be reduced and well productivity increased.

## INTRODUCTION

Peroxydisulfate salts (persulfates) are one of the most common oxidizers used during hydraulic fracturing treatments for proppant pack cleanup. Persulfates are capable of producing free radicals by several different mechanisms. In hydraulic fracturing, we primarily rely on heat to homolytically cleave the persulfate ion into two sulfate free radicals.' These free radicals seek electrons to balance an unpaired electron.

The free-radical oxidation of hemiacetals is a chain reaction. The process begins when free radicals are generated. Sulfate free radicals extract a hydrogen atom by attacking the 1-4 b-glycosidic linkages of the mannose backbone and the 1-6 a-glycosidic linkages to the pendant galactose substituents. Breaking these linkages reduces the polymer molecular weight. It is also possible to break the carbon-oxygen bond in the cyclic hemiacetal structure, although that reaction is less favorable.

The free-radical attack on the polymer turns the polymer into a free-radical molecule. These unstable free-radical species then split into two smaller molecules, one of which remains a free radical. That free-radical segment can either extract hydrogen from another polymer molecule or fragment into smaller molecular segments, creating another free radical. This ongoing process is referred to as fragmentation and propagation. The process ends when two free radicals combine, enabling the unpaired electrons to become paired and returning the molecule to a low energy state (termination step).

The result of oxidative polymer degradation is viscosity and molecular-weight reduction.[2] Degrading the polymer molecular weight enables reservoir fluids to displace the fracturing fluid from the proppant pack more easily,[3,4] resulting in higher conductivity proppant packs.[5,6]

During the treatment, polymer is concentrated in the fracture to a level many times higher than in the fracturing fluid by the fluid leakoff process.[5,7] The concentrated polymer requires high breaker concentrations to achieve good proppant pack cleanup (see Fig. 1). Yet the fluid rheology suffers if too much live active breaker is added to the fluid (see Fig. 2). The paradox is that active breaker concentrations high enough to improve proppant-pack conductivity will reduce the fluid

viscosity too quickly for efficient fracture creation and effective proppant placement in most treatments. Thus, it is necessary to retard or delay the oxidizer reaction.

## ENCAPSULATED BREAKERS

**A** wide variety of methods can reduce the rate of reaction between the polymer and the oxidizer. Some of these methods — referred to here as encapsulation — are:

- encapsulating active ingredients in impermeable membranes that release breakers when crushed[8,9]
- encapsulating active ingredients in an impermeable membrane or coating that dissolves and releases the active ingredients[10,11]
- encapsulating active ingredients in semipermeable membranes that rupture (and release active ingredients) by osmotic swelling[12]
- encapsulating active ingredients in permeable membranes or coatings that allow slow active-ingredient release by dissolution of the active chemical through a porous membrane[13]
- forming the chemical into a granular form that has a low dissolution rate[14]
- placing the active ingredient in a porous matrix (porous grain) so that the active ingredient is released by hindered dissolution from the porous grain"
- encapsulating the active ingredients in a material that will erode away from the active ingredient, thereby releasing it into the environment[16]
- forming a microemulsion that contains an aqueous form of the active ingredients, which hinders the diffusion of the active ingredients throughout the fluid"
- forming a macroemulsion in which the dissolved aqueous active ingredients are dispersed within a continuous, immiscible phase.[18]

The only encapsulated breaker studied during this investigation is composed of an oxidizer substrate, ammonium peroxydisulfate (APS), encapsulated in a thin impermeable polymer coating. The coating is designed to release the oxidizer when the encapsulated breaker particles are crushed by the proppant pack during closure. The material is proven to be effective for improving well productivity when applied properly.[19,20] Previous investigations identify two precrush release mechanisms: mechanical release and hydrostatic release.

**Mechanical Release.** Mechanical release results from coating damage as the breaker is mixed and pumped through pumps, blenders, valves, chokes and tubing. Mechanical release was studied using a large-scale flow loop. The breaker and proppant were blended with an aqueous fracturing fluid and then pumped through a high-pressure triplex pump, 50 ft [15.24-m] of 3-in. [$7.6 \times 10^{-2}$-m] inner diameter treating iron, a 5/8-in. [$1.6 \times 10^{-2}$ m] choke, and 1800 ft of 2-in. [$5.1 \times 10^{-2}$-m] inner diameter tubing. Samples collected after the triplex pump and at the end of the tubing indicate that less than 2% of the encapsulated breaker was prematurely released by the mechanical release mechanism.[21]

**Hydrostatic Release.** Hydrostatic release occurs after the breaker particles are added to water. The chemical breaker leaks through coating imperfections at low hydrostatic pressure. Application of hydrostatic pressure heals the imperfections and reduces the breaker release rate. Fig. *3* illustrates the healing of coating imperfections by applying moderate hydrostatic pressure. The results of this investigation into the effect of temperature, pressure and pH on the hydrostatic release rate are shown here.

## EXPERIMENTAL PROCEDURE

A high-pressure flow-through apparatus was built for this investigation. The apparatus consists of a high-pressure syringe pump, a hot oil bath and a backpressure regulator. Fig. 4 is a schematic of the apparatus. The sample cell is made of 1/4-in. [$6.4 \times 10^{-3}$-m] diameter and 1.5-in. [$3.8 \times 10^{-2}$-m] long stainless steel tubing, and the rest of the tubing is 1/8-in. [$3.2 \times 10^{-3}$-m] diameter. The high-pressure pump can pump against up to 10,000 psig [69-MPa] of pressure. The test procedure was as follows:

1. Preheat the oil bath to the test temperature.
2. Weigh out *0.5* g of the encapsulated breaker (approximately 1000 particles). Carefully place the breaker into the sample cell made of 1/4 in. x 1.5 in. [$6.4 \times 10^{-3}$-m x $3.8 \times 10^{-2}$-m] stainless steel tubing.
3. Install screen made of 100 mesh SS 316 into the reducer at the base of the sample cell. Install the sample cell in the system.

4. Begin injecting deionized water into the system at 5 mL/min using the syringe pump. Fill the tubing with deionized water at ambient pressure. For high-pH experiments, adjust the deionized water with sodium hydroxide. For low-pH experiments, lower the pH of deionized water with acetic acid. Apply the hydrostatic pressure by pumping against a back pressure regulator.

5. Continue injecting water at 5 mL/min. Collect samples every 10 min. Record the exact volume of each sample.

Deionized water was pumped continuously through the sample holder. Water goes through a 5-ft [1.5-m] long heat exchanger upstream of the sample. The APS released from the encapsulated breaker particles by the hydrostatic release mechanism are transported in the flowing water through a cooling bath and into the collection flask. The residence time from the sample cell to the cooling bath is about 2 min.

Two analytical methods, Ultraviolet-Visible (UV-VIS) spectroscopy and Inductively Coupled Plasma (ICP) were used to determine the amount of APS in the samples. UV-VIS can detect APS concentration directly. The analysis involves reacting persulfate ions with iodide in a pH 6.85 buffer to form iodine:

$$S_2O_8^{2-} + 2I^- = I_2 + 2SO_4^{2-} \quad \text{.....} \quad (1)$$

The resulting number from $I_2$ is read on a spectrometer, and the sample concentration is determined by the absorbance value. This method is used to detect persulfate in samples for 150°F experiments only. Persulfate undergoes hydrolysis and decomposes into sulfate after APS dissolves in water and, of course, this decomposition rate increases with temperature. Measurable persulfate decomposition occurs before the sample reaches the cooling bath above 175°F, and the persulfate released cannot be quantified by the UV-VIS method alone. Thus, for experiments at 175°F and above, ICP was used to determine the total APS in samples. ICP detects sulfur, and the total APS concentration can be calculated by the following equation:

$$C_{APS} \times \frac{MW_{APS}}{2MW_S} = C_S \times 3.56 \quad (2)$$

where

$C_{APS}$ = total concentration of APS in ppm
$C_S$ = concentration of sulfur detected by ICP in ppm
$MW_{APS}$ = molecular weight of APS = 228.21 g/mol
$MW_S$ = molecular weigh of sulfur = 32.07 g/mol

The mass of APS detected in each water sample was added to the previous samples to determine the total mass of APS released. The hydrostatic release curve was generated by plotting the cumulative percentage of APS released from the sample cell as a function of time.

## RESULTS AND DISCUSSION

Encapsulated APS with a 22%-by-weight coating was used for this study. Tests were performed at 150°F, 175°F, 200°F and 225°F, 0 to 8000 psig [0 to 55-MPa], and pH of 4, 7 and 9.5.

**Hydrostatic Pressure.** Pressure has a significant impact on the hydrostatic release rate at elevated temperature. Figs. 5 through 8 are the results of 150°F, 175°F, 200°F and 225°F hydrostatic release tests, respectively. The APS release rate at 150°F was weakly influenced by pressure. Increasing hydrostatic pressure reduced the APS release rate at 175°F and above. The APS releases at 175°F after 2 hours for 0 psig [0-MPa], 500 psig [3-MPa], 2000 psig [14-MPa] and 8000 psig [55-MPa] are 35%, 19%, 8% and 7%, respectively. After 4 hours, the releases for these pressures are 78%, 66%, 33% and 12%. At 225°F, the pressure impact is more significant at earlier time. The releases are 62%, 40% and 12% at 500 psig, 2000 psig and 8000 psig after 60 minutes. After 3 hours, the releases are 87%, 78% and 70% at 500 psig, 2000 psig and 8000 psig.

**Temperature.** Figs. 9 through 12 show the hydrostatic-release-rate dependence on temperature at fixed pressures. The temperature impact is most significant at lower pressure. At 0 psig, the three release curves depart right after 10 minutes for 150°F, 175°F and 200°F, indicating early APS release (225°F was not tested at 0 psig). After 1 hour, the releases at 150°F, 175°F and 200°F are 3.7%, 13% and 90%. At 8000 psig, the temperature impact was more significant at later time. After 60 minutes, the releases are 3.7%, 4.4%, 5% and 12% at 150°F, 175°F, 200°F and 225°F, respectively. After 4 hours, the releases are 6.8%, 12%, 24% and 80% at these four temperatures.

The initial release rates and the departure times, calculated at each temperature and pressure, are shown in Table 1. The departure time is the time at which the breaker release rate increases substantially above its initial rate. The initial release rate increases with increasing temperature and decreasing pressure.

**pH**. A few experiments were performed to determine the impact of fluid pH on the hydrostatic release rate. The experiments were carried out at 175°F and 225°F. The results, shown in Figs. 13 and 14, indicate that pH has a negligible effect on the hydrostatic release rate.

**Correlating Experiments to Downhole Conditions.** Correlating the encapsulated breaker hydrostatic release during low-pressure experiments to the actual hydrostatic release under high-pressure downhole conditions facilitates better use of encapsulated breakers and improves proppant pack cleanup. The maximum allowable breaker concentration is the concentration at which hydrostatic release reduces the fluid viscosity to the minimum allowable for successful proppant placement (with whatever safety margin is called for). To correlate the performance of encapsulated breakers from low-pressure rheology experiments to downhole pressure conditions, use the experimental data in this document and rheology curves generated from Model 35 and Model 50 rheometers. The equivalent downhole encapsulated breaker concentration, $C_{DH}$, can be expressed as

$$C_{DH} = C_{Test} \times \frac{\%\ \text{Release at Test Pressure}}{\%\ \text{Release during Treatment}} \quad \ldots(3)$$

where $C_{Test}$ is the breaker concentration at test condition and *% Release during Treatment* is the sum of *Downhole Pressure Release* and mechanical release (2%),

$$\%\ \text{Release during Treatment} = \text{Downhole Pressure Release} + 2\% \quad \ldots\ldots\ldots\ldots(4)$$

The maximum allowable breaker concentration can be similarly determined with Eqs. 3 and 4 using the maximum breaker concentration as $C_{Test}$.

## BREAKER SCHEDULE DESIGN

The results suggest that tests evaluating the stability of fracturing fluids at low-hydrostatic-pressure conditions (such as using Model 35 or Model 50 rheometers) do not represent the actual breaker performance under fracturing conditions. Breaker schedules based on these low-pressure tests underuse encapsulated breakers and jeopardize the proppant pack cleanup process.

The optimal breaker concentration should be determined by the following steps:

1. Design fracture treatment.
2. Determine the exposure time and temperature of each stage from the treatment design.
3. Perform rheology tests using several concentrations of encapsulated breaker at the exposure temperature.
4. Determine the maximum allowable breaker concentration for each stage at low pressure (test condition) using rheology data.
5. Determine the percent hydrostatic release at test pressure using the release data.
6. Determine the actual percent hydrostatic release at downhole pressure using the release data.
7. Determine the maximum allowable breaker concentration at downhole pressure using Eq. (3).
8. Determine the most cost-effective breaker concentration by estimating the job cost, the postclosure polymer concentration, the proppant pack conductivity and 1-year production for several breaker concentrations.
9. Determine the optimal breaker concentration, which is the lower of the maximum allowable breaker concentration and the most cost-effective breaker concentration.

A step-by-step example of breaker determination is given in Appendix A.

## CONCLUSIONS

The following conclusions are drawn from this study:

1. The hydrostatic release rate of the encapsulated breaker is a strong function of pressure. The release rate decreases with increasing hydrostatic pressure.
2. The hydrostatic release rate of the encapsulated breaker also strongly depends on the temperature. The release rate increases with increasing temperature.
3. Fluid pH has negligible effect on the hydrostatic release of the encapsulated breaker.
4. Breaker schedules based on low-pressure tests underuse encapsulated breakers since hydrostatic pressure has a

substantial impact on release rate.

5. A step-by-step process is provided to determine optimal treatment breaker concentrations based on low-pressure rheology experiments and fracture design.

## ACKNOWLEDGMENTS

The authors thank Charles Keith for his input and Richard Lake for his help in collecting data for this paper. We also thank Wayne Frenier and Andre Roberson for their kind help with the ICP measurements.

## NOMENCLATURE

$C$ = total concentration of APS, ppm
$C^{APS}$ = equivalent downhole encapsulated breaker concentration, lb/1000 gal [kg/m$^3$]
$C^{DH}$ = maximum allowable breaker concentration at downhole treating pressure, lb/1000 gal [kg/m$^3$]
$C_s^{Max}$ = concentration of sulfur detected by ICP, ppm
$C^{Test}$ = encapsulated breaker concentration used during rheology test, lb/1000 gal [kg/m$^3$]
$MW$ = molecular weight of APS, 228.21 g/mol
$MW^{APS}_S$ = molecular weigh of sulfur, 32.07 g/mol
ppt = pounds of chemical per 1000 gallons of fluid, lbm/1000 gal [kg/m$^3$]

## SUBSCRIPTS

APS = ammonium peroxydisulfate
s = sulfur
DH = downhole conditions
Test = test conditions
Max = maximum allowable

## REFERENCES

1. Huyser, E.S.: *Free-Radial Chain Reactions,* Wiley-Interscience, New York, (1970) 282.
2. *Reservoir Stimulation,* 3rd edition, M. J. Economides, and K. G. Nolte (eds), John Wiley & Sons, LTD, New York, (2000) 8-4.
3. Pope, D.S., Leung, L.K-W., Gulbis, J., Constien, V.G.: "Effects of Viscous Fingering on Fracture Conductivity," *SPE 28511,presented at the SPE 69th Annual Technical Conference and Exhibition,* New Orleans (September 25-28,1994).
4. Voneiff, G.W., Hopkins, C.W., Holditch & Associates, Inc., S.A., Hill, D.G.: "Calculating Benefits of Advanced Stimulation Technologies," *SPE 37934,presented at the SPE Hydrocarbon Economics and Evaluation Symposium,* Dallas (March 16-18, 1997).
5. Brannon, H.D., and Pulsinelli, R.J.: "Breaker Concentrations Required to Improve the Permeability of Proppant-Packs Damaged by Concentrated Linear and Borate-Crosslinked Fracturing Fluids," *SPE Production Engineering,* (November, 1992) 338-342.
6. Gulbis, J., King, M.T., Hawkins, G.W., Brannon, H.D.: "Encapsulated Breaker for Aqueous Polymeric Fluids," *SPE 19433, presented at the SPE Formation Damage Control Symposium,* Lafayette, (February 22-23, 1990).
7. Penny, G.S.: "An Evaluation of the Effects of Environmental Conditions and Fracturing Fluids Upon the Long-Term Conductivity of Proppants," *SPE 16900,presented at the 62""Annual Technical Conference and Exhibition of the Society of Petroleum Engineers,* Dallas, TX (September 27-30, 1987).
8. Nolte, Kenneth G.: "Fracturing Fluid Breaker System Which is Activated by Fracture Closure," *U.S. Patent No. 4,506,734* (March 26, 1985).
9. Seighman, J.T.: "Process for Encapsulating Liquid Acids and Product," *US Patent No. 4,713,251* (December 15, 1987).
10. Nelson, Erik B., Constien, G., Cawiezel, Kay E.: "Delayed Borate Crosslinked Fracturing Fluid Having Increased Temperature Range," *U.S. Patent No. 5,658,861* (August 19, 1997).
11. Alterman, D.S., and Chun, K.W.: "Encapsulation Particles," *U.S. Patent No. 3,983,254* (September 28, 1976).
12. Manalastas, P. V., Drake, E.N., Kresge, E.N., Thaler, W.A., McDougall, L.A., Newlove, J.C., Swarup, V., and Geiger, A.J.: "Breaker Chemical Encapsulated with a Crosslinked Elastomer Coating," *U.S. Patent No. 5,110,486* (May 5, 1992).
13. McDougall, L.A., Newlove, J.C., and Haslegrave, J.A.: "Polymer Article and its Use for Controlled Introduction of Reagent into a Fluid," *U.S. Patent 4,670,166* (June 2, 1987).
14. Song, J.H., Record, D.W., Broderick, K.B., and Sundstrom, C.W.: "Method of Controlling Release of Sucralose in

Chewing Gum Using Cellulose Derivatives and Gum Produces Thereby," *U.S. Patent No. 5,227,182* (July 13, 1993).
15. Won, R.: "Method for Delivering an Active Ingredient by Controlled Time Release Utilizing a Novel Delivery Vehicle Which can be Prepared by a Process Utilizing the Active Ingredient as a Porogen," *U.S. Patent No. 4,690,825* (September 1, 1987).
16. King, M.T.: "Method for Treating Subterranean Formations," *U.S. Patent No. 4,919,209* (April 24, 1990).
17. Hoefner, M.L., and Fogler, H.S.: "Effective Matrix Acidizing in Carbonates Using Microemulsions," *Chemical Engineering Progress,* (May 1985) 40-44.
18. Yan, L., Sullivan, R.B., de Rozieres, J., Gaz, G.L., and Hinkel, J.J.: "An Overview of Current Acid Fracturing Technology with Recent Implications for Emulsified Acids,'' *SPE 26581, presented at the 68th Annual Technical Conference,* Houston (October 3-6, 1993).
19. Small, J., Wallace, M., van How, S., Brown, E., Pferdehirt, D. and Thompson, J.: "Improving Fracture Conductivities with a Delayed Breaker System: A Case History," *SPE 21497, presented at the SPE Gas Technology Symposium,* Houston (January 23-25, 1991).
20. Waters, G.A., and DeLeon, D.D.: "Encapsulated Breakers in the Red Fork Formation of the Anadarko Basin: A Case History," *SPE 25468, presented at the Production Operations Symposium,* Oklahoma City (March 21-23, 1993).
21. Elbel, J., Gulbis, J., King, M.T., and Maniere, J.: "Increase Breaker Concentration in Fracturing Fluids Results in Improved Gas Well Performance," *SPE 21716, presented at the Production Operations Symposium,* Oklahoma City (April 7-9, 1991).

## METRIC CONVERSION FACTORS

| | | | | | |
|---|---|---|---|---|---|
| ft | x | 3.048 | E-01 | = | m |
| cp | x | 1.0 | E-03 | = | Pa*s |
| "F | x | (°F – 32)/1.8 | | = | °C |
| gal | x | 3.785 412 | E-03 | = | $m^3$ |
| in. | x | 2.54 | E+00 | = | cm |
| mL | x | 1.0 | E+00 | = | $cm^3$ |
| psi | x | 6.894 757 | E+00 | = | kPa |

## APPENDIX A—BREAKER OPTIMIZATION PROCEDURE

A step-by-step example for determining the optimal breaker concentration for the Pad stage of a treatment is given below. This process would be applied to each stage of the job.

Step 1: Fig. A-1 is the end-of-job temperature tracking for the Pad. Total pump time is 55 minutes and bottomhole treating pressure is 2000 psig [14-MPa].

Step 2: The exposure time is 55 minutes and exposure temperature is 200°F for this stage.

Step 3: Rheology tests were performed at 200°F and 0 psig (Fig. A-2).

Step 4: The lowest acceptable viscosity is 100 cp [0.1-Pa*s] at 100 $s^{-1}$. Hence, the maximum allowable concentration for this stage is 0.5 lbm APS/1000 gallons of fluid (ppt) [0.06 kg/$m^3$] (Fig. A-2).

Step 5: The percent hydrostatic release at 200°F and 0 psig (test pressure) is 80% (Fig. A-3).

Step 6: The actual percent hydrostatic release at 2000 psig (downhole treating pressure) is 8% (Fig A-3).

Step 7: Maximum allowable breaker concentration ($C_{Max}$) at the downhole treating pressure is 4 ppt [0.48 kg/$m^3$].

$$C_{Max} = 0.5\text{ppt} \times \frac{80\%}{8\% + 2\%} = 4\text{ppt} \quad \text{.....(A-1)}$$

Step 8: The postclosure polymer concentration is estimated. Then, the job cost, retained conductivity and 1-year production are estimated at different breaker concentrations. The maximum net-present value (NPV) occurs with 10.5 ppt [1.3 kg/$m^3$] of breaker (Fig. A-4).

Step 9: The lower of the maximum allowable breaker concentration (4 ppt) and most cost-effective breaker concentration (10.5 ppt) is 4 ppt. Thus, 4 ppt is the optimal breaker concentration for this stage.

Table 1
Initial Hydrostatic Release Rate at Various Times and Temperatures

| Temperature | Hydrostatic Pressure (psig) | Initial Release Rate (g APS/min/g EB)* | Departure Time (minutes) |
|---|---|---|---|
| **150°F** | **0** | 0.000328 | 180 |
| | **500** | 0.000232 | 300 |
| | **2000** | 0.000214 | 300 |
| | **8000** | 0.000178 | 300 |
| **175°F** | **0** | 0.001652 | 50 |
| | **500** | 0.000816 | 100 |
| | **2000** | 0.000532 | 140 |
| | **8000** | 0.000420 | 260 |
| **200°F** | **0** | 0.01906 | 10 |
| | **500** | 0.01298 | 25 |
| | **2000** | 0.00276 | 50 |
| | **8000** | 0.00101 | 100 |
| **225°F** | **500** | 0.0224 | 10 |
| | **2000** | 0.00826 | 25 |
| | **8000** | 0.00402 | 50 |

* grams of ammonium persulfate per gram of encapsulated breaker (EB)

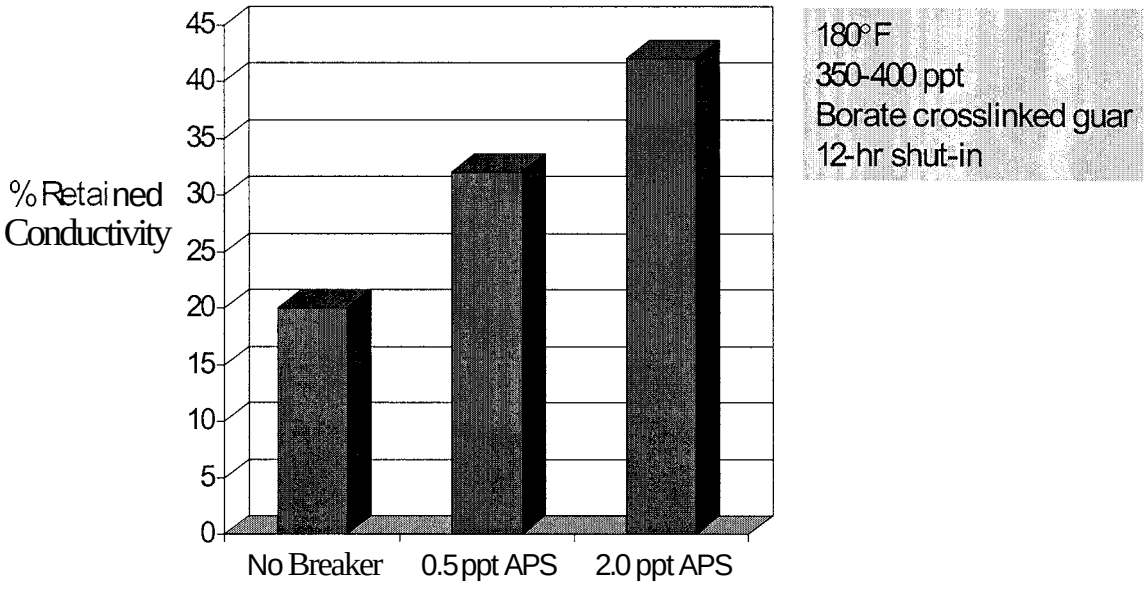


Figure 1 — Effect of APS on Percent Detained Proppant Pack Conductivity

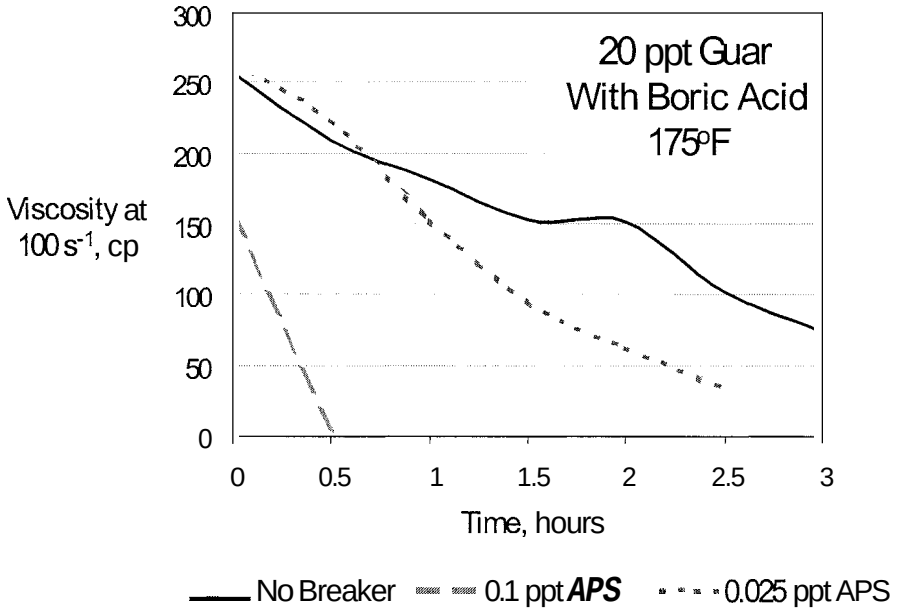


Figure 2 — Effect of Ammonium Persulfate Breaker (APS) on Fluid Rheology

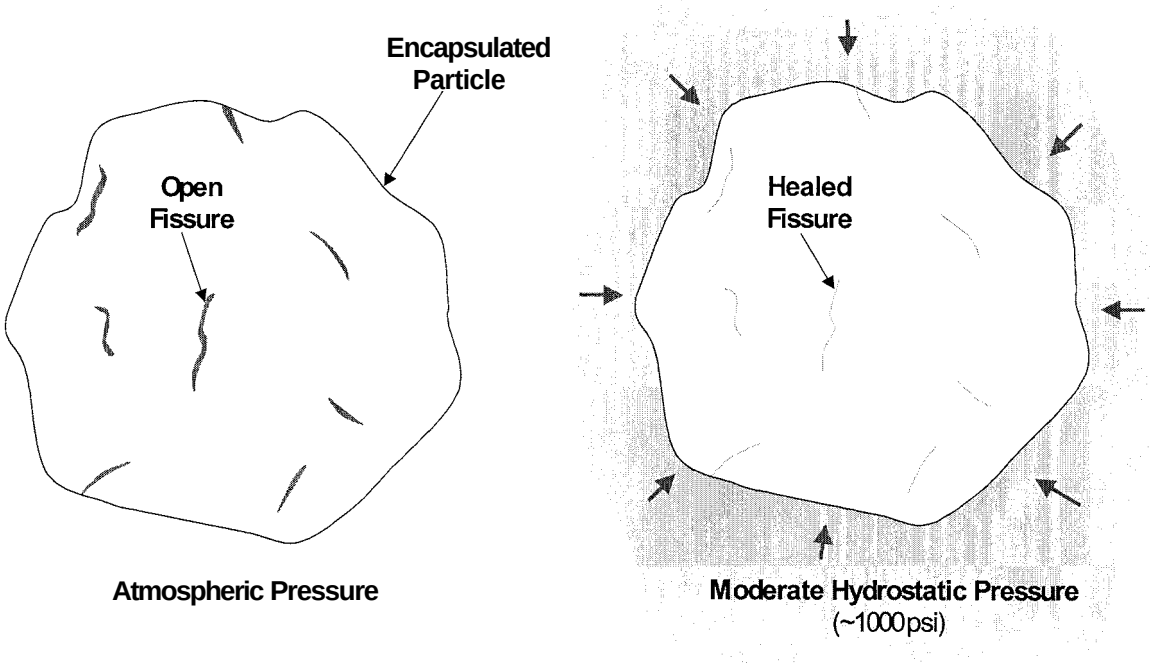


Figure 3 — Breaker Particles Under Atmospheric Pressure and Hydrostatic Pressure
The fissures are partially healed under hydrostatic pressure.

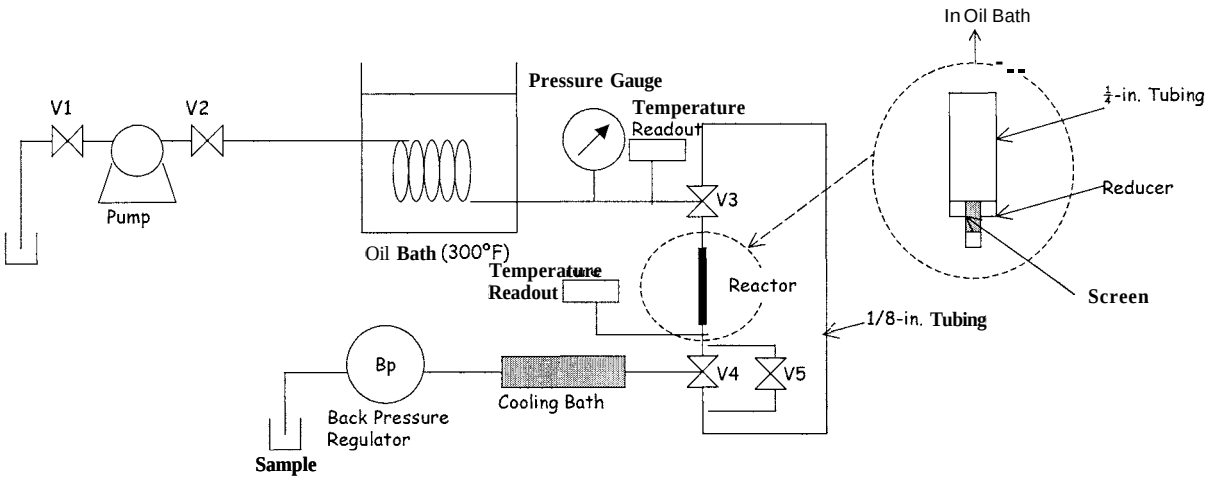


Figure 4 — Schematic of the Breaker Release Apparatus

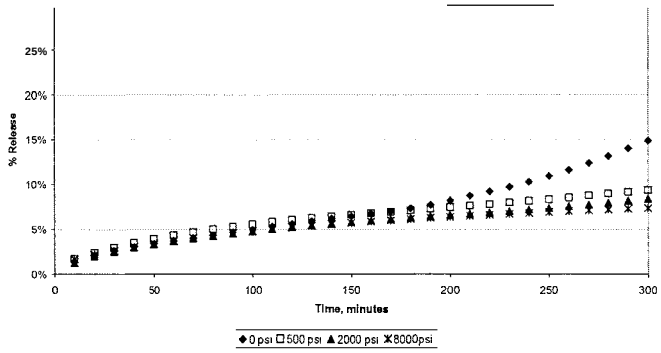


Figure 5 — Hydrostatic Release at 150°F

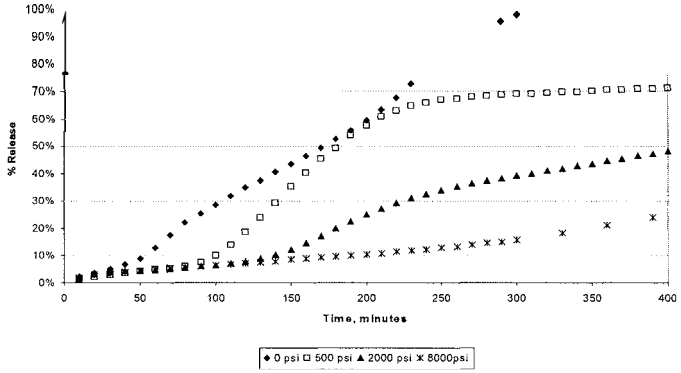


Figure 6 — Hydrostatic Release at 175°F

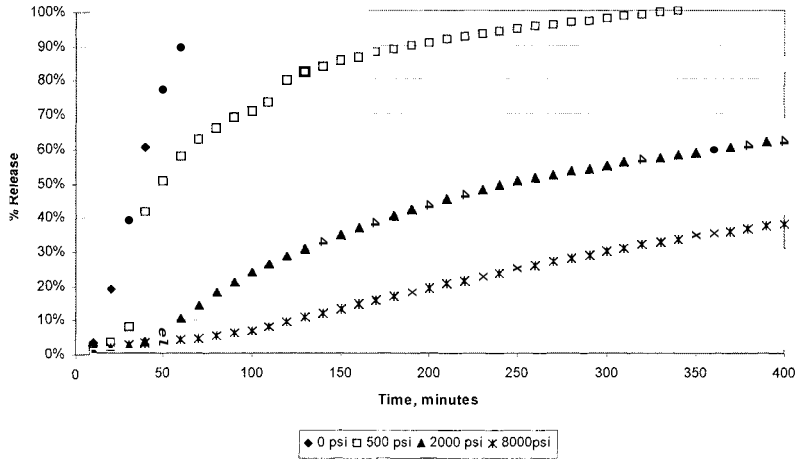


Figure 7 — Hydrostatic Release at 200 F

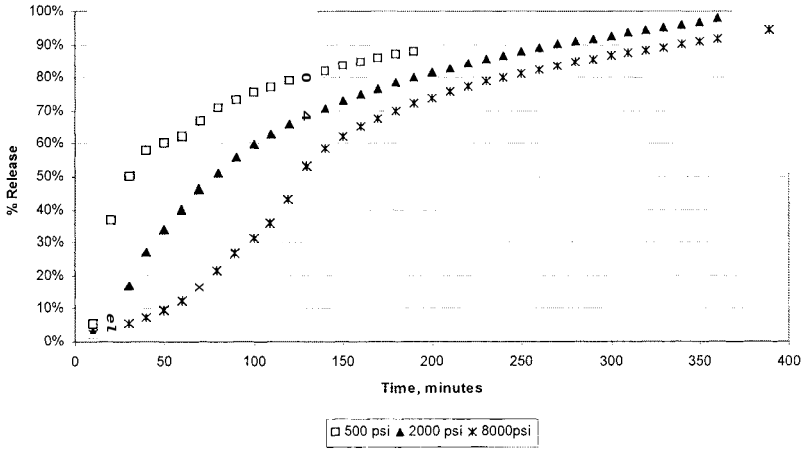


Figure 8— Hydrostatic Release at 225°F

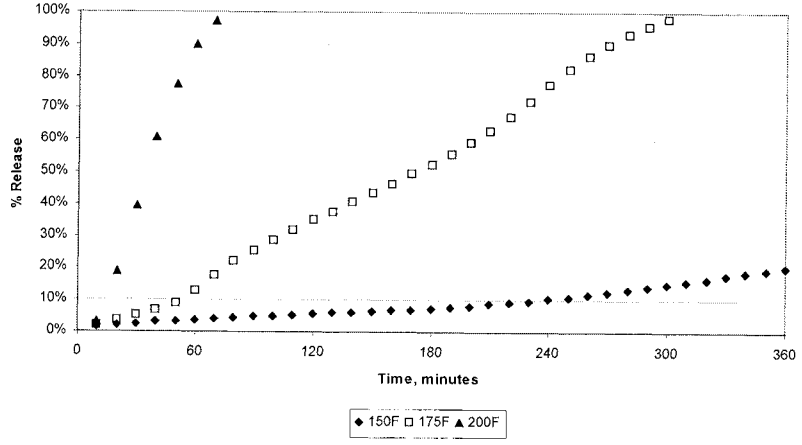


Figure 9 — HydrostaticRrelease at 0 psig

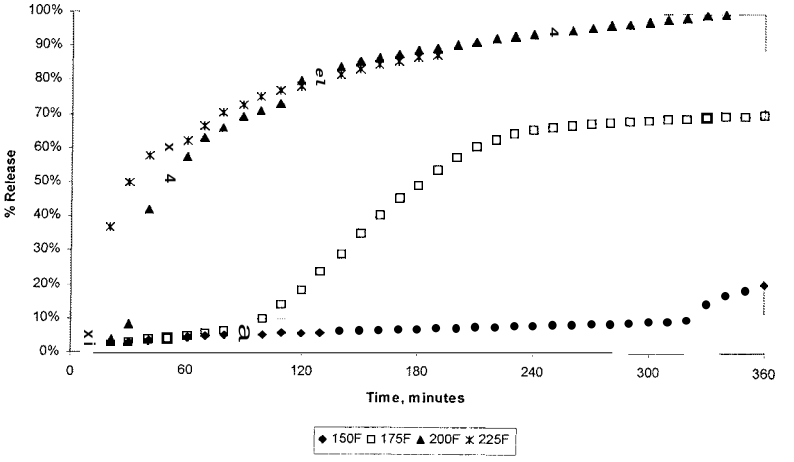


Figure 10 — Hydrostatic Release at 500 psig

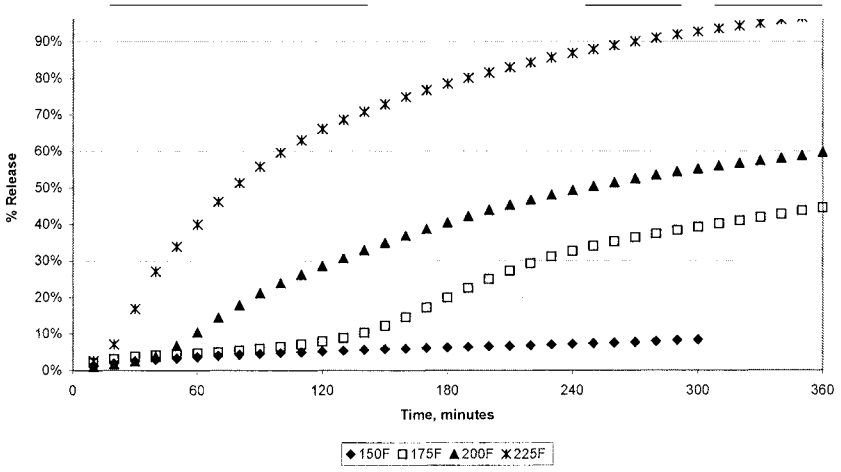


Figure 11 — Hydrostatic Release at 2000 psig

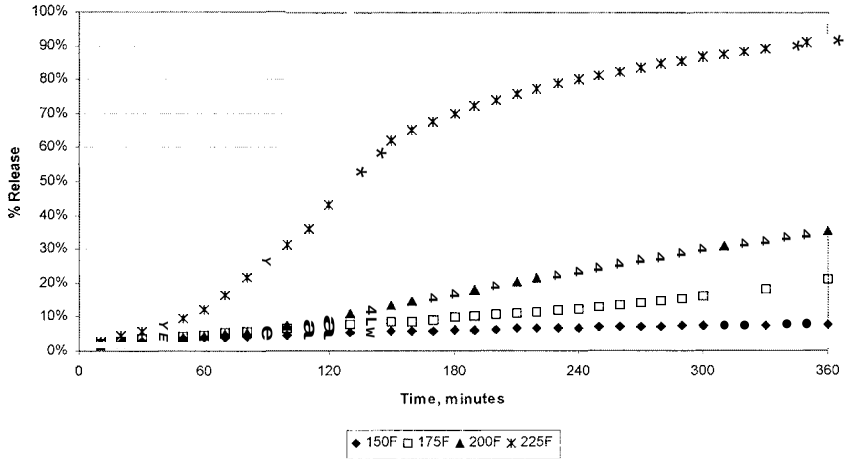


Figure 12 — Hydrostatic Release at 8000 psig

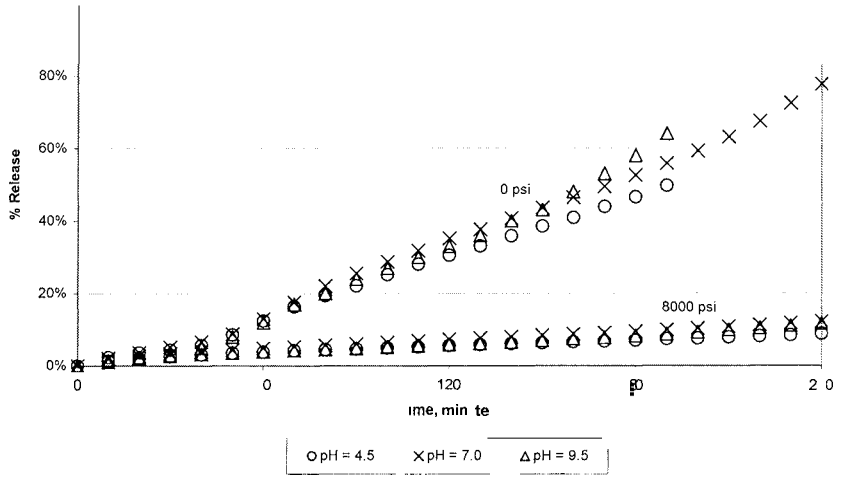


Figure 13 — Effect of Fluid pH on Hydrostatic Release at 175 °F

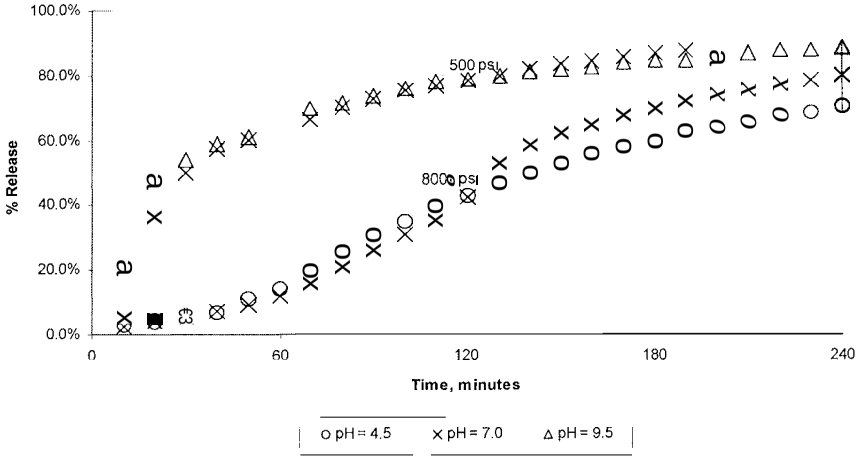


Figure 14 — Effect of Fluid pH on Hydrostatic Release at 225 °F

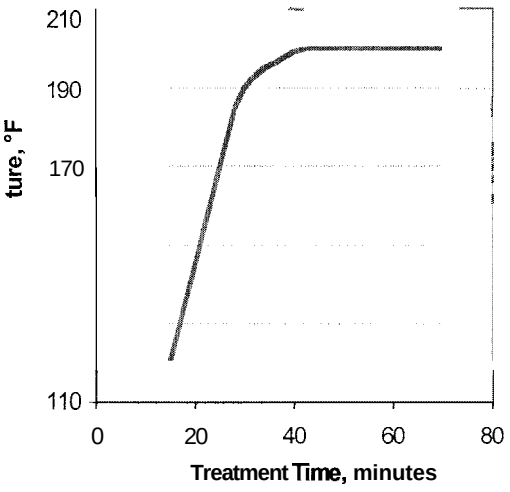


Figure A-I — End-of-Job Temperature Tracking for the Pad Stage

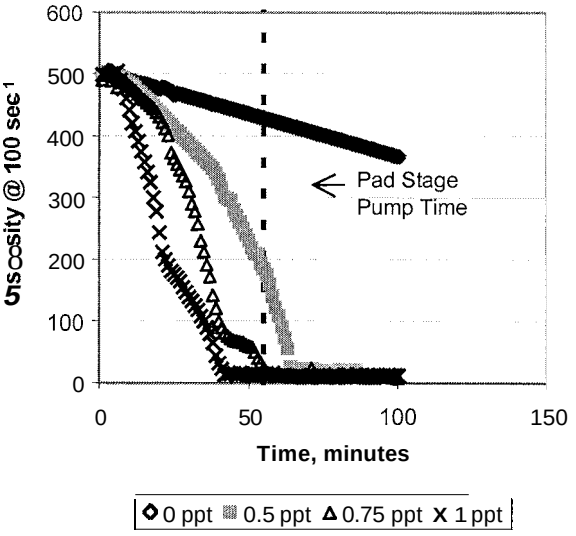


Figure A-2 — Rheology Tests at 200 °F and 0 psi The maximum allowable breaker concentration is 0.5 ppa.

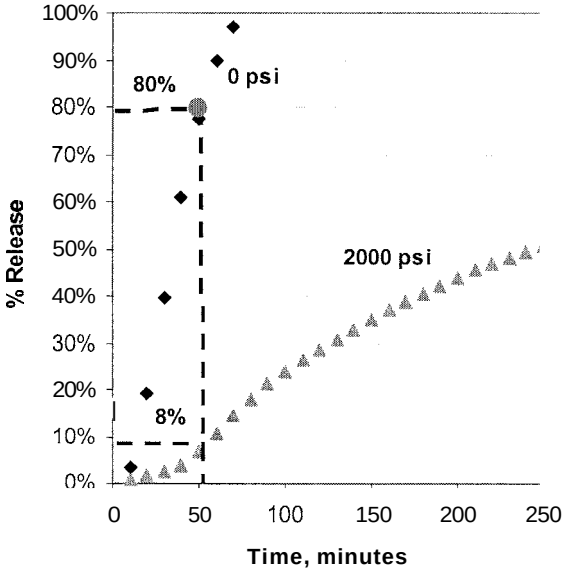


Figure A-3 — Hydrostatic Release at 200 "F- After 55 min, 80% is released at 0 psig and 8% is released at 2000 psi hydrostatic pressure.

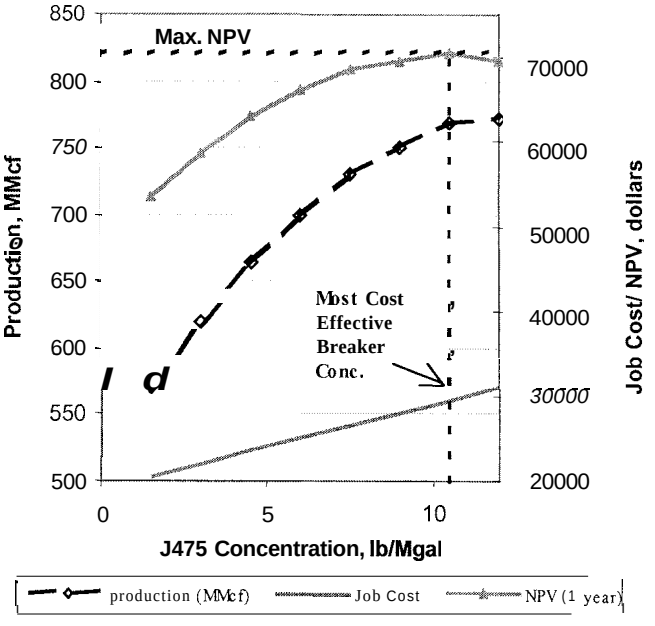


Figure A-4 — Estimate of Most Effective Breaker Concentration